A Study on Design Concept for a Braille Tactile Sensor Segment Using Softness Parameters*

Zhongwei JIANG**, Sayyed Alireza ARABSHAHI** and Tetsuyou WATANABE**

The purpose of this report is to introduce and discuss about the design parameters for a segment of a tactile sensor reading one dot of a Braille alphabet. A sensor segment consisting of a piezoelectric (PVDF) film sandwiched between two elastic materials is designed. Experiments and simulations are used to define and examine the design parameters. With regards to the sensor structure, Free and Clamped boundary conditions are presented and the relevant equations containing the design parameters, e.g. "bending softness", are derived. Applying different materials and thicknesses for layers surrounding the PVDF film, simulations are used to quantize the approximate values for each design parameter. The results show that the output of sensor is mostly dependent on the bending effect near the PVDF layer, and the structure encouraging more bending produces higher output. Finally, it is concluded that the real sensor has a structure which is between Free and Clamped boundary conditions, therefore design parameters are modified to compromise between the two cases and optimum values are presented.

Key Words: Sensor, Finite Element Method, Piezo-Element, Braille, Design Parameters

1. Introduction

Tactile sensors are used in broad area of applications and they have started to open their way into the medical applications[1] including objective diagnostic palpation[2]-[4], rehabilitation applications[5], and even for cosmetics purposes[6],[7]. Though tactile sensors are being used since two decades ago, only few authors[2],[3] have discussed about the design codes and criteria of how a tactile sensor should be.

Considering prostatic palpation, Jiang et al.[2] have designed a diagnostic tactile sensor and have introduced "softness" as a parameter for designing their sensor. Using the concept of "softness", a conceptual design of a tactile sensor was proposed and the influence of geometry and material on the senor performance was examined via simulation[8],[9].

Tactile perception is vital for the blind as Braille alphabet is used for their education. Learning Braille alphabet requires great effort and it takes several years for young children to learn. For elderly people it would be more difficult and they would easily become frustrated. Therefore, it might be convenient for them if an automatic Braille reading system, by which they can understand a Braille text without the requirement of intensive Braille training, were developed[5],[9]. This device can also be used as a useful training aid for the blind to learn Braille alphabet.

Already, some studies have been done on Braille reading machines[10],[11]. Most of them have been focusing on optical character recognition systems using the optical devices such as CCD cameras. These devices have complicated and precise structure including many circuits and cables and more important, their manufacturing costs are high.

Moreover, when using a tactile sensor, the user has to touch directly the Braille. This gives the user a confident as she or he has the superior control over the reading process and, therefore, user's will are respected as well. This is not provided in the optical systems, so a tactile sensor for reading the Braille is required to be developed. Furthermore, the sensor can even be equipped with a haptic perception mechanism providing simultaneous tactile information in addition to the electrical signals.

Using FEA technique, in this paper we try to design a tactile sensor for Braille pattern recognition. FEA is a very powerful and accurate method but it is difficult to in-

* Received 17th October, 2005 (No. 05-4212)

** Faculty of Science and Engineering, Yamaguchi University, 2–16–1 Tokiwadai, Ube 755–8611, Japan.
E-mail: jiang@yamaguchi-u.ac.jp;
e001hn@yamaguchi-u.ac.jp;
t-wata@yamaguchi-u.ac.jp

troduce all details of the structure and materials into the simulation software. So we try to define and find out the important design parameters. With the help of these parameters it would be easier to design a sensor and decide physical parameters such as dimensions and materials for sensor, or to modify the previously designed sensor.

Braille has a precise dot patterns, therefore the sensor can have a simple structure, which in turn, facilitates the definition and deliberating of design parameters. Here, the tactile sensor is imitated by human digital pad and it is composed of a piezoelectric PVDF film as a sensory receptor and soft materials as cutaneous and subcutaneous tissue[6)-9),12]. Starting from a single segment sensor for reading a single dot in Braille alphabet and based on the material and size of the layers surrounding the PVDF film, experiments and simulations are carried out to find out the important parameters as well as the relationship between simulation and experiment.

With regard to the different sensor structures, analytical models are presented and new design parameters, "softness" and "bending softness", are introduced. Further, numerical simulations are used to figure out how the performance of sensor is affected by different boundary conditions and different values for design parameters.

Finally, based on the results obtained by two typical boundary conditions, the consideration on determination of the design parameters is described and confirmed by numerical simulation. The conclusion then reaches that any proposed structure for the real sensor should encourage the bending effect on the layer which is stuck to the PVDF film.

2. Primary Model for Sensor Segment

In this section, based on the experiment results, a calibration factor will be introduced for simulation results. It is obvious that there are many parameters, such as geometry, material and structure of sensor, affecting the sensor output, and it is probable to make enormous combinations of those parameters. Since making a sensor for each combination is almost impossible, we will use numerical methods (the FEM package ANSYS 8.1) to find out the adaptive combination of above-mentioned parameters. Nevertheless, in our previous research[8),9)] we found out that ANSYS produces very high output values when it is used to simulate a sensor with PVDF film. Moreover, the real conditions for experiments can hardly be maintained for simulations, including the real nonlinearity in materials' properties and characteristics of bonding materials (glues). Therefore, we use a calibration factor, by which, we can convert the results of simulation to the real senor output.

2.1 Materials and method

In order to read one Braille dot in one Braille cell, a simple structure for the sensor is proposed in Fig. 1, which is composed of a piezoelectric PVDF film (28 μm) sandwiched between two layers, Medium#1 and #2. Medium#2 is the yardstick layer, made of sponge rubber with $E_2 = 50$ kPa and the thickness of $h_2 = 5$ mm. Two cases are considered for the experiment where in each case the material and the thickness of Medium#1 vary accordingly. This combination is summarized in Table 1, where materials selected for Medium#1 are either OHP sheet or rubber.

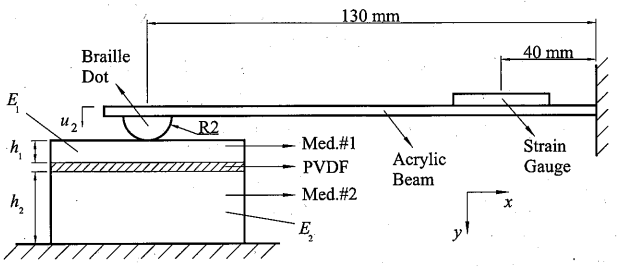

Fig. 1 Schematic diagram of sensor calibrating system

Table 1 Experiment cases

Case	Medium #1	h_1 (mm)	E_1 (MPa)	Medium #2	h_2 (mm)	E_1 (kPa)	u_2 (mm)	p
I	OHP Sheet	0.3	3000	Sponge Rubber	5	5	0.831	288
II	Rubber	1	1	Sponge Rubber	5	5	1.57	385

To make the sensor for experiment, a cut of $16 \times 16\,\text{mm}^2$ of PVDF film is used and placed between the two layers using a spray type glue to form a thin uniform layer of adhesive. Using the two-sided tape, the bottom of sensor is fixed to a hard base. This is schematically shown in Fig. 1. A rigid copper dot, resembling the Braille dot, is attached on an acrylic beam ($E = 2.8$ GPa) with the cross section of height=2 mm and width=9 mm. A strain gauge (KYOWA; KFG-5-120-C1-5), mounted on the acrylic beam, is connected to a digital oscilloscope via a dynamics strain amplifier (KYOWA; DPM-712B). The PVDF film, with bottom grounded, is connected to the same digital oscilloscope. A signal filter/amplifier (NF 3628, 1 Hz~1.59 MHz 48 dB/oct) is placed before the oscilloscope where all signals pass through a 60 Hz lowpass filter. The signals captured in the oscilloscope are further introduced into a PC and processed by Matlab (Math Works).

Since the overall height of sensor during the experiment vary from case to case, the beam is adjusted in the way that it has always been in contact with the surface of sensor. The beam tip over the Braille dot is pushed gently by hand on to the sensor to avoid imposing any impulse effect on the senor. It has been tried that the pressing of the dot over the sensor follows the same pattern. Each case is carried out 10 times within a 10-second window of time. The average deflection of the beam tip, u_2, for each case is presented in Table 1. Figure 2 shows the output signals

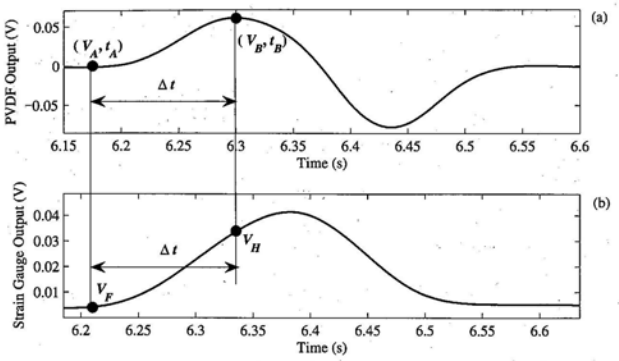

Fig. 2 PVDF sensor and strain gauge outputs used for normalization

for case II, where Fig. 2 (a) and (b) corresponds to PVDF and strain gauge outputs respectively during the time of experiment.

In the next step, simulation is carried out. The same sensor, which was used in experiment, is modeled using ANSYS 8.1. Also the same combinations (Table 1) are applied for simulation. The Braille dot in the simulation is pushed down according to u_2, based on Table 1, over the Braille cells. In the simulation the Braille dots are also considered as rigid and the whole simulation is done under transient static method and with contact analysis (during the time where Effectors are indented by the Braille dots).

2.2 Normalization and calibration factor

To understand the relationship between the experiment and simulation, the output of PVDF film should be normalized in either one. In general, the output of a piezoelectric material depends on the amount of displacement and the time that this happens. The voltage difference, $V_B - V_A$, for PVDF film is the difference between the maximum and minimum, points A and B respectively in Fig. 2, which is obtained at the time interval of Δt. However, it was found that Δt is almost the same for Case I and II. Therefore, the PVDF output can only be normalized by pushing (indentation) displacement. The beam tip displacement is obtained from the signal of strain gauge, $V_H - V_F$ (which is proportional to u_2), as shown in Fig. 2. Therefore, the normalized output voltage can be presented as:

$$D = \frac{V_B - V_A}{u_2} \tag{1}$$

Note that Eq. (1) is also used in the simulation to normalize the PVDF output.

Figures 3 and 4 show the results of experiment and simulation respectively for different cases, with the lateral axis showing the experiment and simulation cases (see Table 1) and the vertical axis representing the normalized output of the PVDF film. Both figures show the same trend for the PVDF output but the simulation results by ANSYS has much higher voltage values. Therefore, the calibration factor, p, corresponding experiment and simulation results

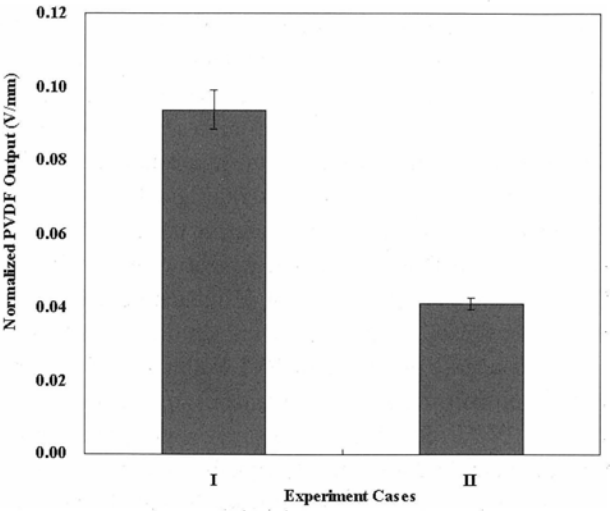

Fig. 3 Normalized output from experiment

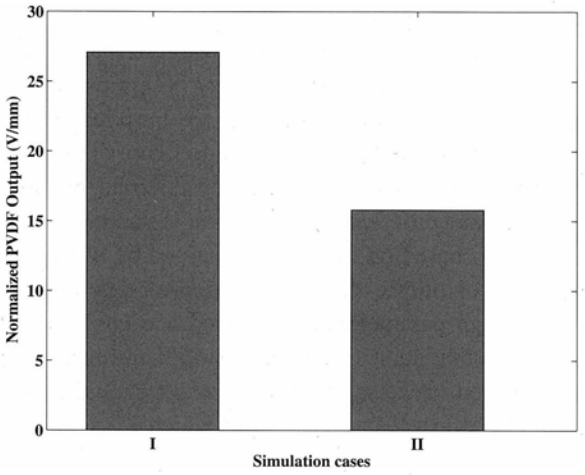

Fig. 4 Normalized output from simulation

can be defined as:

$$p = \frac{D_{Simulation}}{D_{Experiment}} \tag{2}$$

From Table 1, the average value would be $p = 337$. This value will be used hereinafter to calibrate the simulation results.

3. Analytical Model

From the results of Fig. 3 or Fig. 4 and Table 1, with free boundary condition on sidelines, the performance of the sensor segment is understood to be corresponding to the thickness and Young's modulus of the surrounding materials. If one considers the results of these two figures, then from Table 1 a conclusion for geometry and material arrangement of the sensor can be derived for this specific design, i.e., with this design of sensor the material in Medium#1 should be "harder" and "thinner" than Medium#2. Based on this comparative description, it is possible to define the "index of thickness", f, as the ratio of thickness between Medium#1 and #2,

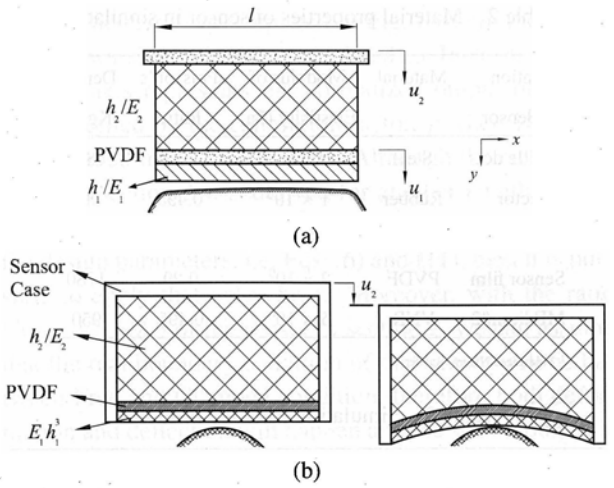

Fig. 5 Analytical model for (a) Free BC and (b) Clamped BC (pushed u_2 in y direction)

$$f=\frac{h_1}{h_2} \tag{3}$$

The same way, "index of modulus", e, is defined as the ratio of Young's modulus of Medium#1 and #2,

$$e=\frac{E_1}{E_2} \tag{4}$$

From the previous experiments the question may rise that how the thickness and Young's modulus affect the sensor output. To answer this, consider the model presented in Fig. 5 (a), where no constraint is applied on the sidelines of the sensor and it is pushed with the amount of u_2 over a contact surface.

Based on this model and with regard to human's touch sense, while neglecting the pushing area on the sensor, Jiang et al. defined the softness as[2],

$$S_i=\frac{h_i}{E_i} \tag{5}$$

where i represents the Medium number. Note that, this parameter combines the geometry and material property into one single parameter.

Now, considering the pushing area in a two-dimensional problem, it is obvious that the sensor length affects the deflection of layers. So, the "softness" of Eq. (5) is better to be modified by:

$$S_i=\frac{h_i}{lE_i} \tag{6}$$

where, l is the length of sensor.

Using S_i and the above equations, the deflections, δ_i, at ith layer (for $i=1,2$) become:

$$\delta_1=u_2\frac{\alpha_1 S_1}{S_1+S_2} \quad \text{and} \quad \delta_2=u_2\frac{\alpha_2 S_2}{S_1+S_2} \tag{7}$$

where α_i are coefficients corresponding to the material properties such as Poisson's ratio, the size of sensor and boundary conditions. The output of PVDF film which is related to the deflections of Medium#1 and #2 can be written as:

$$\begin{cases} V\propto\delta_1 = u_2\alpha_1 S_A & \text{if } S_2\gg S_1 \\ V\propto(\delta_1+\delta_2) = u_2(\alpha_1 S_A+\alpha_2 S_B) & \text{if } S_1\approx S_2 \\ V\propto\delta_2 = u_2\alpha_2 S_B & \text{if } S_1\gg S_2 \end{cases} \tag{8}$$

in which

$$S_A=\frac{1}{1+S_2/S_1} \quad \text{and} \quad S_B=\frac{S_2/S_1}{1+S_2/S_1} \tag{9}$$

Equation (8) with regard to Fig. 5 (a) implies that the output of the sensor depends on S_i and the sensor geometry. That is, if Medium#2 is a soft material the strain developed in the PVDF film follows the strain produced in Medium#1 and vice versa. Although the above model can show clearly the relation between "softness" and sensor output, there is a limitation for that model where the contact area is considered to be flat. Therefore, it might not be true when the sensor is touching the Braille dot in practical use.

To solve these problems, in this paper we introduce another model, based on another type of structure of sensor segment. This idea comes from the fact that the sensor touches a protruded object, such as a Braille dot, so the layers of Medium#1 and PVDF film can experience bending. In real applications, the sensor is enclosed by a compartment to protect it and to provide facilities for mounting on the human's finger and wirings, with the sides of sensor glued to the sensor case. This is illustrated in Fig. 5 (b) where a sensor segment is shown before and after pushing over a protruded surface. Under these circumstances, the strain developed in PVDF film is generated due to the bending. Consequently, Medium#1 and PVDF film can be considered as a beam anchored to the sidelines of the case; which becomes Clamped BC.

The deflection in a simply supported beam is proportional to:

$$\delta\propto\frac{l^3}{48EI} \tag{10}$$

where l and I are the length of sensor and moment of inertia respectively.

Obviously, the idea for "softness" should consider the bending deflection. Here, we introduce "bending softness", S_{1b}, for Medium#1 as,

$$S_{1b}=\frac{l^3}{E_1h_1^3} \tag{11}$$

therefore, the sensor output related to the deflection can be written as:

$$V\propto\delta\equiv\beta S_{1b} \tag{12}$$

where β is the coefficient related to the piezoelectric constants and material properties.

4. Single Segment Simulation

4.1 Segment design and definitions

In the previous section two models were analyzed. The coefficients in Eqs. (8) and (12) affect greatly the sensor performance since they are related to the material

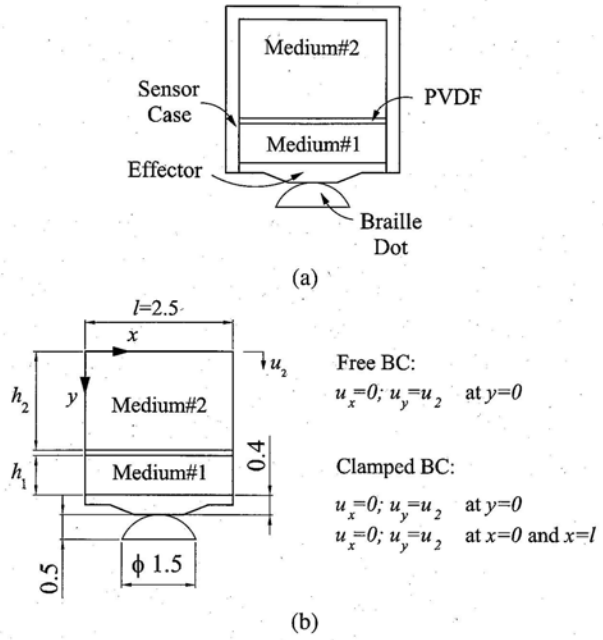

Fig. 6 Proposed sensor segment, (a) structure and (b) geometry

properties (other than thickness and Young's modulus) and sensor structure. Moreover, it was not clear what range of material, with what dimensions, can be suitable for the real sensor. Therefore, hereinafter, a sensor segment will be introduced based on the two boundary conditions and simulations will be carried out to find the optimum values for the design parameters.

The proposed structure of segment is shown in Fig. 6 (a). It is the same as Fig. 1 expect that an additional protruded layer, namely surface Effector, is added beneath Medium#1. It is supposed that the Effector will contact the Braille dot when the sensor is positioned properly over a Braille cell. To construct the FEM model, the Braille dot geometry is simplified and based on the concept proposed in Fig. 6 (a), the geometry of the sensor segment can be recommended by Fig. 6 (b). Due to the dimension of the Braille dots and the distance between them[13], the overall length of the segment is almost fixed and cannot vary much. It is assumed that our segment might be enclosed in the sensor compartment (and an array of them will form a sensor unit); therefore the length of segment becomes $l = 2.5$ mm.

The case of segment is replaced by the appropriate boundary conditions. Two boundary conditions are assumed to be valid for the sensor design, as discussed in previous section, and are shown in Fig. 6 (b). In Free BC, only the base of Medium#2 is connected to the sensor case and all the sidelines ($x = 0$ and $x = l$) are set to be free. In Clamped BC, both the base line of Medium#2 and the sensor sidelines are glued to the sensor case. Therefore, when the sensor is pushed with the distance of u_2 in y direction, both the base and sidelines undertake the same displacement in y direction while they are restricted to move in x direction.

Table 2 Material properties of sensor in simulation

Location on Sensor	Material	Modulus of Elasticity (Pa)	Poisson's Ratio	Density (Kg/m^3)
Braille dots	Steel	200×10^9	0.28	7850
Effector	Rubber	1×10^6	0.495	900
Medium#1	VNR[1]	5×10^6	0.495	950
Sensor film	PVDF	2×10^9	0.29	1780
MEdium#2	VNR	5×10^6	0.495	950

[1] Vulcanized Natural Rubber

Table 3 Simulation table for Free BC

Case	h_1 (mm)	E_1 (MPa)	h_2 (mm)	E_2 (MPa)	f	e	S_1 (10^{-6}/Pa)	S_2 (10^{-6}/Pa)	S_2/S_1
$F_{BC}1$	0.8	5	2	5	0.4	1	0.064	0.16	2.5
$F_{BC}2$	2	5	2	5	1	1	0.16	0.16	1
$F_{BC}3$	4	5	2	5	2	1	0.32	0.16	0.5
$F_{BC}4$	0.8	5	2	0.05	0.4	100	0.064	16	250
$F_{BC}5$	2	5	2	0.05	1	100	0.16	16	100
$F_{BC}6$	4	5	2	0.05	2	100	0.32	16	50

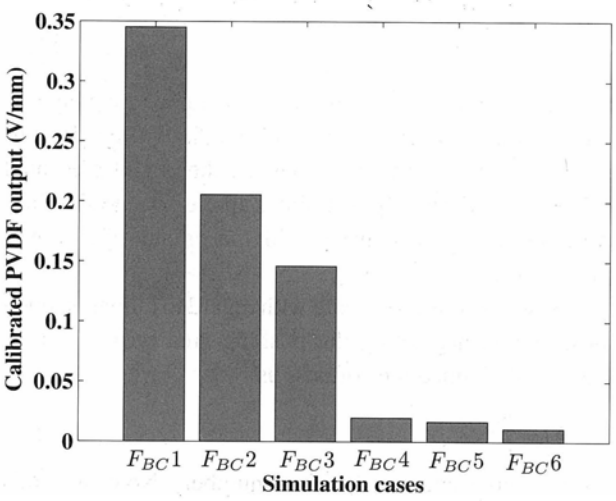

Fig. 7 Simulation results for Free BC

The materials selected for simulation of the sensor are listed in Table 2. The sensor in the simulation is pushed $u_2 = 0.3$ mm down over the Braille dot. Same as previous section, the whole simulation is done under transient method using the contact analysis during the period when Effector touches the Braille dot.

4.2 Results

The first series of simulations are carried out under Free BC, with variation of parameters h and E as summarized in Table 3, where F_{BC} stands for Free BC. Here, E_2 is selectable by 0.05 or 5 MPa, and h_1 will be 0.8, 2 or 4 mm respectively. The material of Medium#1 and thickness of Medium#2 are selected as the yardstick values in the simulation, with $E_1 = 5$ MPa and $h_2 = 5$ mm respec-

tively. The results are depicted in Fig. 7 where the lateral axis shows simulations cases related to Table 3, and the vertical axis represents the normalized output of PVDF film modified by the calibration factor, p, (i.e. $\mathcal{V} = D/p$) as described in Eqs. (1) and (2). Although the calibration factor in section 2 was derived for another length of sensor, but since the effect of length is already included in the design parameters, i.e. Eqs. (6) and (11), then it is possible to apply that value here. Moreover, with the ratio $l/(h_1+h_2) > 2.5$ of the sensor in section 2, we can assume that the real boundary condition of that sensor will be between Free and Clamped condition, therefore both deformation and deflection will happen and the sensor output is related to both.

The results show that the PVDF output does not correspond to bending. Instead, it corresponds to the lateral deformation in x direction. One reason is the ratio of $l/(h_1+h_2)$ (Fig. 6(b)), which varies $0.5 < l/(h_1+h_2) < 1$. That means the length of sensor is smaller than, but near its height. The second reason is boundary condition. Together they cause the whole sensor to act like a block under a bulk deformation. Especially the boundary condition does not encourage any bending and even if bending happens, this is due to the small thickness of Medium#1 and the shape of Braille dot. Under Free BC, the material property seems to be a dominant parameter since it has stronger influence than thickness.

As the first three cases of the results show, the sensor gives higher output when $S_2/S_1 \approx 1$. That means in Eq. (8) the condition of $S_2 \approx S_1$ provides the maximum output in the equation. The physical interpretation of the above condition is that, when a Free BC is used for the sensor segment, both Medium#1 and #2 can have the same material but with Medium#1 thinner than Medium#2 the output will be improved.

Now, back to Eq. (8), if $S_2/S_1 \gg 1$, then the output of the sensor is related to Medium#1 which becomes rigid, and since little deflection occur in Medium#1, the sensor output will be reduced. This is in agreement with the results shown in Fig. 7 for the last three cases. As for $S_2/S_1 \ll 1$, the output of the sensor will be reduced as Medium#2 acts like a rigid body.

Comparing the simulation results and the estimation from Eq. (8), one can say, although Eq. (8) is derived for a planar contact condition between the sensor and an object, it can be used for a protruded object, such as a Braille dot, with a good approximation.

For the second series of simulations assume that the sensor has a Clamped BC (Fig. 6 (b)) with the combination of materials and geometry as represented in Table 4, where C_{BC} stands for Clamped BC. The results are depicted in Fig. 8. Unlike Free BC, the results show that due to the applied structure, the PVDF output is improved and has higher output values. As we explained in the analytical model, the sensor output corresponds to the bending and the deflection of PVDF film; the higher the deflection the higher the output is. This indicate that, the "bending softness" S_{1b}, described by Eq. (11), could be a design parameter and the "bending softness" of PVDF film $S_{Pb} = l^3/E_p h_p^3$ could be neglected if $S_{1b} \ll S_{Pb}$, where $S_{Pb} = 356 \times 10^{-6}\text{Pa}^{-1}$ in the present simulation.

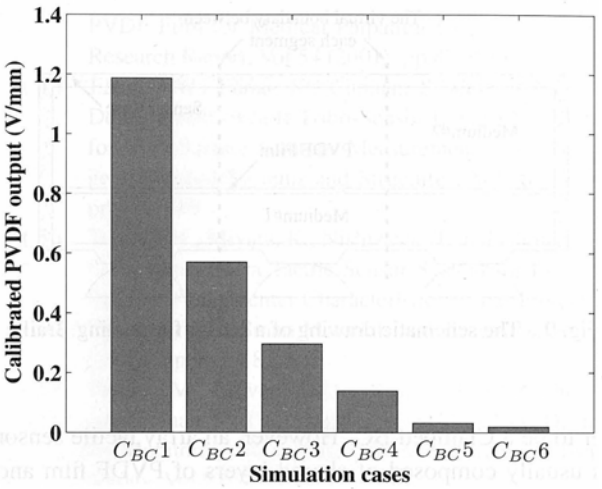

Fig. 8 Simulation results for Clamped BC

Table 4 Simulation table for Clamped BC

Case	h_1 (mm)	E_1 (MPa)	h_2 (mm)	E_2 (MPa)	f	e	S_{1b} (10^{-6}/Pa)	S_2 (10^{-6}/Pa)
$C_{BC}1$	0.8	5	2	0.05	0.4	100	5.2	16
$C_{BC}2$	0.8	5	2	5	0.4	1	5.2	0.16
$C_{BC}3$	2	5	2	0.05	1	100	0.39	16
$C_{BC}4$	2	5	2	5	1	1	0.39	0.16
$C_{BC}5$	4	5	2	0.05	2	100	0.048	16
$C_{BC}6$	4	5	2	5	2	1	0.048	0.16

Two combinations can be noted from Table 4 and Fig. 8. At first, considering case $C_{BC}1$ and 3 (where $S_2 = 16 \times 10^{-6}\text{Pa}^{-1}$ is identical), the output of the sensor in case $C_{BC}1$ ($S_{1b} = 5.2 \times 10^{-6}\text{Pa}^{-1}$) is higher than case $C_{BC}3$ ($S_{1b} = 0.39 \times 10^{-6}\text{Pa}^{-1}$). Second, looking at the case $C_{BC}1$ and $C_{BC}2$ (where $S_{1b} = 5.2 \times 10^{-6}\text{Pa}^{-1}$ is identical), when Medium#2 becomes softer ($S_2 = 16 \times 10^{-6}\text{Pa}^{-1}$ in case $C_{BC}1$), the sensor output becomes higher than the case with harder Medium#2 ($S_2 = 0.16 \times 10^{-6}\text{Pa}^{-1}$ in case $C_{BC}2$). It is clear that, when deriving Eq. (12), we have neglect the influence of Medium#2, which acts as a soft elastic foundation, because it is relatively smaller than the one of Medium#1. From the simulation results, the overall conclusion for Clamped BC can be summarized, saying that Medium#1 should be relatively thinner and harder than Medium#2.

4.3 Discussion

The above simulations discuss the sensor segment with two typical boundary conditions. Obviously, it can be concluded that the ideal structure for the sensor is bet-

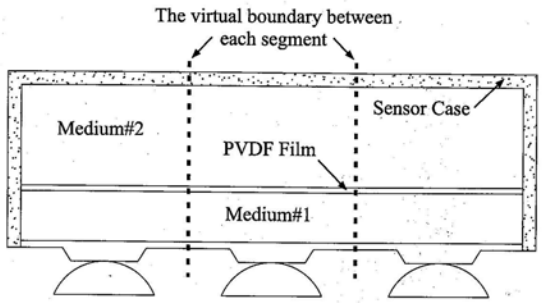

Fig. 9 The schematic drawing of a sensor for reading Braille

ter to be a Clamped BC. However, an array tactile sensor is usually composed of shared layers of PVDF film and different media[9],[14],[15] and one may think that the virtual segments are connected together to form the sensor as depicted in Fig. 9. Therefore, the boundary condition between segments is believed to be something between Free and Clamped conditions. But, as Figs. 7 and 8 represented, the output level between Free and Clamped BC varies a lot and it is necessary to compromise the design parameters in a way that the output of each BC becomes reasonable. This is due to the nature of the sensor output which is related to both deflection and deformation. To set up a criterion, we assume wherever the sum of voltages in Free and Clamped BC was smaller than 50 mV (or 0.17 V/mm with pushing distance of $u_2 = 0.3$ mm) the signal would be difficult to be acquired by a single AD convertor and treated in data processing due to the ratio of noise to signal.

Referring to Figs. 7 & 8 and with regard to Tables 3 & 4, we mainly discuss three situations, $C_{BC}1$ & $F_{BC}4$, $C_{BC}2$ & $F_{BC}1$ and $C_{BC}4$ & $F_{BC}2$, where each pair has the same materials but different boundary conditions. Their sums of calibrated sensor output voltage are $V_{F_{BC}} + V_{C_{BC}} =$ 363 mV (1.21 V/mm), 275 mV (0.915 V/mm) and 105 mV (0.35 V/mm) respectively at pushing distance of 0.3 mm. All outputs are higher than 50 mV as we were expected.

Now, first comparing $C_{BC}1$ & $F_{BC}4$ with $C_{BC}2$ & $F_{BC}1$, their difference is just on the parameter S_2, the softness of Medium#2. It is indicated clearly that with an increase of S_2, i.e. the softer Medium#2, higher output in clamped BC but lower output in Free BC are obtained. However, if the Medium#2 is selected to be too soft, the sensor structure should be designed in a complete Clamped or simply supported boundary condition, and the reaction force will be too small to counteract the deflection of Medium#1 back.

In case of $C_{BC}1$ & $F_{BC}4$ and with the parameter $S_2 = 16 \times 10^{-6}\text{Pa}^{-1}$, the estimated reacting forces at pushing distance of $u_2 = 0.3$ mm are 0.6 N and 14 N for $F_{BC}4$ and $C_{BC}1$ respectively. The reacting force in Free BC is too small to push the Medium#1 back after the release of the touch force. If one decreases the parameter S_2, to $0.8 \times 10^{-6}\,\text{Pa}^{-1}$ (for example rubber with $E_2 = 1$ MPa), the

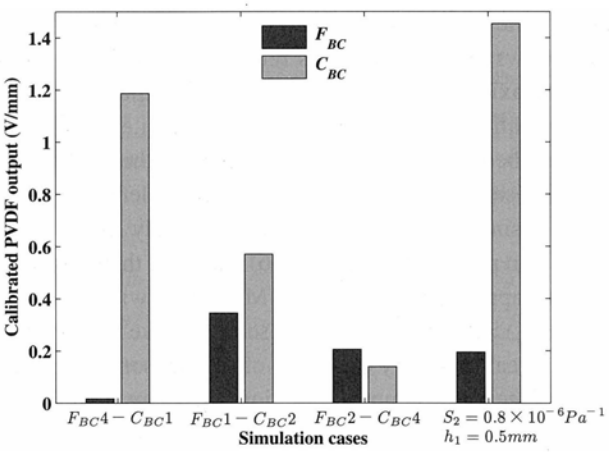

Fig. 10 Selected simulation results and the results with $S_2 = 0.8 \times 10^6\,\text{Pa}^{-1}$ and $h_1 = 0.5$ mm

reacting force will be increased to 4.6 N and 15.2 N for $F_{BC}4$ and $C_{BC}1$ respectively.

Next, compare $C_{BC}2$ & $F_{BC}1$ with $C_{BC}4$ & $F_{BC}2$, where only the parameter h_1, the thickness of Medium#1, is changing in which, $h_1 = 0.8$ mm and 2 mm corresponding to $S_1 = 0.064$ and 0.16, $S_{1b} = 5.2$ and $0.39 \times 10^{-6}\,\text{Pa}^{-1}$ respectively. As Figs. 7 and 8 show, the sensor outputs in both free and Clamped BC become higher if h_1 goes smaller, i.e. when S_1 decreases and S_{1b} increases. However, since $S_{1b} \ll S_{Pb}$, then in the design of a sensor "bending softness" should be satisfied by $S_{1b} < S_{Pb}/10 = 35.6 \times 10^{-6}\,\text{Pa}^{-1}$. If one sets $h_1 = 0.5$ mm (which satisfies the above condition), the softness of Medium#1 will be $S_1 = 0.04 \times 10^{-6}\,\text{Pa}^{-1}$ and $S_{1b} = 25 \times 10^{-6}\,\text{Pa}^{-1}$ for Free and Clamped BC respectively, and it will satisfy the mentioned criteria.

Based on the above discussion, the results of simulation with $S_2 = 0.8 \times 10^{-6}\text{Pa}^{-1}$, $S_1 = 0.04 \times 10^{-6}\text{Pa}^{-1}$ and $S_{1b} = 25 \times 10^{-6}\text{Pa}^{-1}$ under Free and Clamped boundary conditions, are depicted in Fig. 10. The calibrated output voltages, for Free and Clamped BC are $V_{F_{BC}} =$ 57 mV ($\mathcal{V}_{F_{BC}} = 0.19$ V/mm) and $V_{C_{BC}} = 435$ mV ($\mathcal{V}_{C_{BC}} =$ 1.45 V/mm) at the pushing distance of $u_2 = 0.3$ mm respectively. The estimated reaction force for Free BC is 4.5 N and for Clamped BC is 16.7 N.

The results show that in both boundary conditions the overall sensor output has been improved. Specially in Clamped BC, although S_2 has been reduced, but bending is encouraged by increasing S_{1b}. For Free BC, when comparing to $F_{BC}4$ case, both reducing S_2 and S_1 have lead to higher output.

Since the output of sensor corresponds strongly to the bending, in the design of sensor, it is necessary to prepare a structure which encourages the bending effect. Obviously, any values that are presented for design parameters will be affected by manufacturing techniques such as bonding condition between different layers.

5. Conclusion

In this paper a single sensor segment for reading one dot of Braille character is modeled and the softness design parameters are proposed and discussed. At first, experiments were used to calibrate the results of FEM models with the contact simulation. In order to easily understand how the different layers and structures of the sensor affect the sensor performance, two parameters, "softness" and "bending softness", were introduced.

For Free BC model, the "softness" defined by Jiang et al.[2] was redefined and the strain developed on the PVDF film was found to be mainly affected by the bulk strain of surrounding layers. Unlike Free BC, in Clamped BC, the PVDF output is mostly corresponded to the strain developed during the bending of the film, and thus it was related to the "bending softness".

Simulations were carried out with different softness values. For Free BC, as the analytical model predicted, it was understood that with the approximately the same "softness" values of Medium#1 and #2, the output of sensor would be higher. For clamped BC, higher output values were obtained when "bending softness" in Medium#1 and "softness" in Medium#2 took higher values, as expressed by the due analytical model.

Finally, it was explained that the real sensor has a boundary condition which is a combination of both Free and Clamped BC and the values for "softness" and "bending softness" were modified so the sensor can provide high enough output for both boundary conditions.

With the different simulations carried out here, it was proved that the concept of softness is valid for the design of sensor. Therefore, the method presented in this paper can be used for the design of this kind of tactile sensors by considering the provisions for appropriate bending of the PVDF film and material arrangements. Then it would be possible to put segments together, and with a proper structure, a complete sensor can be made.

References

(1) Lee, M.H. and Nicholls, H.R., Review Article—Tactile Sensing for Mechatronics—A State of the Art Survey, Mechatronics, Vol.9, Issue 1 (1999), pp.1–31.

(2) Jiang, Z.W., Chonan, S., Tanahashi, Y., Tanaka, M. and Kato, T., Development of Soft Tactile Sensor for Prostatic Palpation Diagnosis: Sensor Structure Design and Analysis, Shock and Vibration, Vol.7 (2000), pp.67–79.

(3) Jiang, Z.W., Development of Soft Tactile Sensor Using PVDF Film for Medical Palpation Diagnosis, Toyota Research Report, Vol.54 (2001), pp.87–97.

(4) Jiang, Z.W., Funai, K., Chonan, S. and Tanaka, M., Development of Soft Tribo-Sensor Using PVDF Film for Skin Surface Contour Measurement, J. of Intelligent Material Systems and Structures, Vol.10 (1999), pp.481–488.

(5) Tanaka, M., Miyata, K., Nishizawa, T. and Chonan, S., Development of a Tactile Sensor System for Reading Braille: Fundamental Characteristics of the Prototype Sensor System, Smart Materials and Structures, Vol.14 (2005), pp.483–487.

(6) Tanaka, M., Lé vêque, J.L., Tagami, H., Kikuchi, K. and Chonan, S., The "Haptic Finger" —A New Device for Monitoring Skin Device, Skin Research and Technology, Vol.9 (2003), pp.131–136.

(7) Tanaka, M., Sugiura, H., Lé vêque, J.L., Tagami, H., Kikuchi, K. and Chonan, S., Active Haptic Sensation for Monitoring Skin Condition, J. of Materials Processing Technology, Vol.161 (2005), pp.199–203.

(8) Arabshahi, S.A. and Jiang, Z.W., Fundamental Study on Design of a Braille Tactile Sensor, Proceedings of the First International Conference on Complex Medical Engineering CME2005, May 15–18, (2005), pp.122–127.

(9) Arabshahi, S.A. and Jiang, Z.W., Development of a Tactile Sensor for Braille Pattern Recognition: Sensor Design and Simulation, Smart Materials and Structures, Vol.14 (2005), pp.1569–1578.

(10) Oyama, Y., Tajima, T. and Koga, H., Character Recognition of Mixed Convex-Concave Braille Points and Legibility of Deteriorated Braille Points, Systems and Computers in Japan, Vol.28, No.2 (1997), pp.44–53.

(11) Antonacopoulos, A. and Bridson, D., A Robust Braille Recognition System, Lecture Notes in Computer Science, Vol.3163 (2004), pp.533–545, Springer-Verlag GmbH.

(12) Miyata, K., Tanaka, M., Nishizawa, T. and Chonan, S., Wearable Sensor System for Reading Braille Using Neural Networks, Proceedings of the First International Conference on Complex Medical Engineering CME2005, May 15–18, (2005), pp.134–139.

(13) Kazuka, Y., (in Japanese), (1999) http://www.econ.keio.ac.jp/staff/nakanoy/article/braille/BR/index.html

(14) Yu, K.H., Kwon, T.G., Yun, M.J. and Lee, S.C., Development of a Tactile Sensor Array with Flexible Structure Using Piezoelectric Film, KSME International Journal, Vol.16, No.10 (2002), pp.1222–1228.

(15) Yu, K.H., Yun, M.J., Kwon, T.G. and Lee, S.C., Distributed Flexible Tactile Sensor, International Journal of Applied Electromagnetics and Mechanics, Vol.18 (2003), pp.53–65.